

Instruction-Guided Scene Text Recognition

Yongkun Du¹, Zhineng Chen^{1*}, Yuchen Su¹, Caiyan Jia², Yu-Gang Jiang¹

¹School of Computer Science, Fudan University, China

²School of Computer and Information Technology, Beijing Jiaotong University, China

{ykdu23, ycsu23}@m.fudan.edu.cn, {zhinchen, ygj}@fudan.edu.cn, cyjia@bjtu.edu.cn

Abstract

Multi-modal models have shown appealing performance in visual tasks recently, as instruction-guided training has evoked the ability to understand fine-grained visual content. However, current methods cannot be trivially applied to scene text recognition (STR) due to the gap between natural and text images. In this paper, we introduce a novel paradigm that formulates STR as an instruction learning problem, and propose instruction-guided scene text recognition (IGTR) to achieve effective cross-modal learning. IGTR first generates rich and diverse instruction triplets of $\langle \text{condition}, \text{question}, \text{answer} \rangle$, serving as guidance for nuanced text image understanding. Then, we devise an architecture with dedicated cross-modal feature fusion module, and multi-task answer head to effectively fuse the required instruction and image features for answering questions. Built upon these designs, IGTR facilitates accurate text recognition by comprehending character attributes. Experiments on English and Chinese benchmarks show that IGTR outperforms existing models by significant margins. Furthermore, by adjusting the instructions, IGTR enables various recognition schemes. These include zero-shot prediction, where the model is trained based on instructions not explicitly targeting character recognition, and the recognition of rarely appearing and morphologically similar characters, which were previous challenges for existing models.

1. Introduction

Scene text recognition (STR) is a longstanding computer vision task that focuses on reading natural text images. Essentially, it learns a mapping from the image modality to the text modality, aiming to decipher the character sequence. In the past few years, researchers have recognized that STR methods go beyond visual recognition, and have developed many elegant ways to incorporate information of other modalities [3, 13, 43, 53, 61].

*Corresponding Author

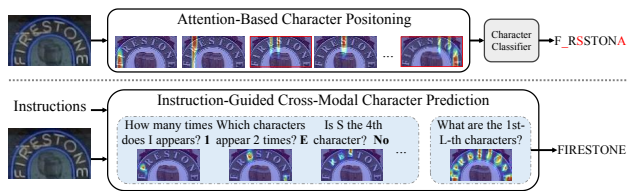


Figure 1. **Upper:** popular attention-based STR models follow the pipeline of extracting features of every character and then classifying them. Mis-recognitions may happen if features are positioned incorrectly. **Bottom:** IGTR first performs character attribute prediction with instructions, which aims at text understanding. Then it is trained to predict characters with recognition instructions.

Recently, there is a trend to develop vision-and-language approaches [25, 30, 32, 52] for the execution of generic visual tasks [15, 33]. Notably, pioneering models such as Grounding-DINO [32] and SAM [25] have embraced the integration of language as instructive guidance. This integration facilitates a profound understanding of fine-grained visual content, e.g. a specific attribute of object *the left lion* rather than a *lion*, surpassing the performance of uni-modal models in downstream tasks [15, 33].

Similarly, STR models could also be assisted in recognizing text if equipped with the ability to thoroughly understand the visual content of a text image. However, achieving this presents a challenge when trivially applying existing instruction schemes [25, 30, 32, 52] to STR. This challenge arises from the distinct nature of text images, wherein the predominant visual content is characterized by a sequence of characters rather than various objects and scenes. In light of this, we argue that the goal of deeply understanding text images can be attained by considering character-specific attributes such as character frequency, distribution patterns, positional relationships, etc. Consequently, we propose formulating instructions as character-level question-answer pairs as detailed in Tab. 1. Each question is tailored to a specific character attribute, guiding the model to learn these attributes. For instance, when examining the *FIRESTONE* image at the bottom of Fig. 1, humans effortlessly grasp

Condition	Condition Option	Question	Answer	Task
1. Character $\{C_i\}$ in the image 2. Character $\{C_i\}$ appear $\{N_i\}$ times 3. The i -th character are C_i 4. Sub-string $\{C_s - C_{s+m}\}$ in the image 5. There are L characters in the image 6. None	1/2/3/4/5/6	How many times does A appear in the image?	2	Statistics
	1/2/3/4/5/6	How many times does A appear in the first 3 characters?	1	Constraint statistics
	1/2/3/4/5/6	Does A appear 2/1 times in the image?	Yes/No	Check statistics
	1/2/3/4/5/6	Does A appear 2/1 times in the first 3 characters?	No/Yes	Check constraint statistics
	1/2/3/4/5/6	Which character in the image is A ?	1st,6th	Character search
	1/2/3/4/5/6	Is A the 1-st/5-th character in the image?	Yes/No	Check character search
	1/2/3/4/5/6	Which characters appear 2 times?	A and T	Reverse statistics
	1/2/3/4/5/6	Which characters appear 1 time in first 3 characters?	A, R and E	Constraint Re-statistics
	1/2/3/4/5/6	Where is the sub-string RTE/RTS ?	2nd/None	Sub-string match
	1/2/3/4/5/6	Is sub-string RTE at position 2/3?	Yes/No	Check sub-string match
1/2/3/4/6	How many characters in the image?	6	Length prediction	
4/6	What are the first and last characters?	A/A	Pre-task identification	

Table 1. Character attribute prediction instructions (taking *ARTETA* as the example), where **red** in *Question* column denotes character or numerical variables. Different colors in *Task* column represent different question tasks. The same below.

Recognition Condition	Recognition Question	Answer	Task
None	What are the 1-st to L-th characters in the image?	$C_1 - C_L$	Parallel decoding recognition
1-st to i -th characters are $C_1 - C_i$	What is the $i+1$ -th character?	C_{i+1}	Auto-regressive recognition
1-st to $i-1$ -th, $i+1$ -th to j -th characters are known	What is the i -th character?	C_i	Re-identification
There is a sub-string $C_i - C_j$	What is the next/previous character of the sub-string?	C_{i-1}/C_{j+1}	Extrapolating recognition

Table 2. Text recognition instructions. Text recognition tasks are marked by cyan.

the character attributes and promptly respond to the posed questions. Evidently, if STR models could mimic human understanding, they could precisely recognize text.

Motivated by this observation, we propose instruction-guided scene text recognition (IGTR), employing instructions in the format of $\langle condition, question, answer \rangle$ to guide effective text image understanding and recognition. Firstly, we generate a diverse set of instructions by condition-question-answer triplets encompassing character statistic, search, sub-string matching, and their inversions (refer to Tab. 1). Then, we formulate a set of recognition instructions with the same triplet pattern explicitly tailored for text recognition (see Tab. 2). Secondly, we devise a dedicated architecture for cross-modal instruction learning and prediction. This architecture features an innovative cross-modal feature fusion module designed to assimilate the requisite multi-modal features from the provided condition, question and image embeddings. Additionally, it incorporates a multi-task answer head responsible for addressing diverse questions and recognizing the text. For the successful completion of the task corresponding to each instruction, it is imperative that the IGTR model possesses a profound understanding of character properties, consequently achieving superior text recognition.

IGTR represents a novel paradigm in STR. As shown in Fig. 1, unlike existing models that mostly follow the pipeline of extracting features corresponding to every character and then classifying them, IGTR attains a comprehensive understanding of text image content through in-depth

exploration of character attributes, subsequently achieving precise predictions via recognition instructions.

We conduct extensive experiments on English and Chinese benchmarks. The results show that IGTR outperforms existing models significantly in terms of accuracy. Meanwhile, it enjoys remarkable modeling flexibility inherited from the instruction-guided nature. Even when trained solely on character attribute prediction without using explicit recognition instructions, the model exhibits impressive zero-shot prediction capability. Moreover, by adjusting the instructions accordingly, IGTR demonstrates superior performance in recognizing both rarely appeared and morphologically similar characters. Contributions of this paper are summarized as follows.

- We propose IGTR that regards STR as a cross-modal instruction learning task. Unlike existing models, IGTR facilitates accurate text recognition by understanding text images, presenting a novel paradigm for STR.
- We introduce rich and diverse instruction triplets $\langle condition, question, answer \rangle$ and develop a dedicated architecture to effectively process these instructions, providing the first instruction-guided STR solution.
- Through extensive experiments, we demonstrate the effectiveness of IGTR not only in public benchmarks, but also in providing a uniform framework to flexibly tackle several typical challenges in STR.

2. Related Work

Instruction-guided visual recognition. Multi-modal visual recognition models [15, 33] have received widespread attention recently, due to their ability to understanding fine-grained visual content. As the initial, CLIP [42] and ALIGN [21] performed cross-modal contrastive learning on billion-level image-text pairs, enabling open-set image classification. Later, GLIP [30] and Grounding-DINO [32] introduced instruction-guided object detection, understanding freeform text instructions and detecting objects accordingly. Similar approaches were explored in image segmentation, such as the well-regarded SAM [25] and SegGPT [52]. These models leverage rich interactive instructions such as clicks, boxes, masks and text to achieve generic and deep visual understanding, enabling segmentation of anything. Instruction-guided pipelines have also been applied to tasks like license plate recognition [37] and speech recognition [26]. However, they are more like applications of VQA models [2, 51] or generative models [9, 60] dedicated to these tasks. At present, instruction-guided schemes or multi-modal models suitable for STR are still unexplored.

Scene text recognition (STR). Typically, STR employs an encoder-decoder framework [7, 54] and roughly follows the pipeline: extracting features for every character, then classifying them. There are two major recognition schemes. One is CTC-based [11, 19, 44]. They extract features according to preset stripes, and map each feature to a unique character. The characters are then optimized by the CTC rule [16].

The other is attention-based methods that leverage attention to position every character. Following the success in NLP [46], auto-regressive (AR) methods [27, 29, 43, 45] were introduced to STR. They utilized previously decoded characters as linguistic clues to assist recognition. However, their inference speed was slow, and might suffer from the problem of attention drift for highly deformed text [58]. To mitigate attention drift, some methods [49, 58, 61] proposed to utilize the position clue. Meanwhile, permuted and bidirectional recognition are developed [3, 4], providing a stronger linguistic prior. On the other hand, parallel decoding (PD) models [12, 13, 41, 53, 56, 59], which inferred all characters at once, were developed to seek accurate and fast STR. These methods utilized context information, such as knowledge distillation [41], language models [13, 53, 59], and character counting [12], to compensate for character mis-focusing, as it is challenging to accurately position all the characters in a single forward. Although notable progress made, existing models might not well response to the detailed questions as shown in Tab. 1, as they were optimized at the character sequence level. This motivated us to explore the instruction-guided solution.

3. Method

3.1. Overview

The architecture of IGTR is depicted in Fig. 2. We take *ARTETA* as an example to illustrate it. First, text *ARTETA* is fed into the instruction generation module, where a set of $\langle condition, question, answer \rangle$ instructions is generated following the preset patterns as shown in Tab. 1 and Tab. 2. Then, a subset of them is randomly sampled and fed into an instruction encoder to generate condition and question embeddings. Meanwhile, image embeddings are extracted from an image encoder. Subsequently, these embeddings are fed into a cross-modal feature fusion module (CMFF) to absorb answer-related cross-modal features. In the following, the absorbed embeddings are forwarded to a multi-task answer head and every task is responsible for answering a different type of question, ranging from character attribute prediction to recognition.

3.2. Instruction Generation and Sampling

As shown in Tab. 1 and Tab. 2, we propose a series of character attribute prediction instructions and recognition instructions. Each instruction consists of *condition*, *question* and *answer*, where *condition* is the text information given in advance and *question-answer* indicates the corresponding question-answer pair.

We first introduce the instruction in Tab. 1, whose *condition* is as follows. Take also *ARTETA* as an example, we get three sets of pairwise character attributes. They are: $\{ \langle C_i, N \rangle \}$ describes the existence of character C_i , i.e., with elements $\langle A, 1 \rangle, \langle B, 0 \rangle$, etc. $\{ C_i - N \}$ indicates the occurrence times of appeared character C_i , i.e., with elements $A-2, E-1$, etc. $\{ N - C_i \}$ tells the position of appeared character C_i , i.e., with elements $1-A, 2-R$, etc. By filling in the corresponding attributes, the first three conditions in Tab. 1 can be given. The fourth condition is described as $C_s - C_{s+m}$, where s is the start index and m is length. The fifth condition is fixed and L is the text length.

Then to *question* and *answer*. The question-answer pair is written using either the formats above or the format plus with certain constraints. For instance, the first question-answer pair in Tab. 1 can be written as $A-2$, where A and 2 are the question and answer. The second pair is $A \in [1,3]-1$, where $A \in [1,3]$ is a compound question composed of a raw question and its constraint. All questions in Tab. 1 can be similarly written in this manner. Meanwhile, not all conditions are compatible with the questions, and Tab. 1 gives their compatible options. In addition, the task of each question and their types are also highlighted in Tab. 1.

As for the recognition instruction in Tab. 2, each instruction corresponds to a specific recognition scheme. The first two are equivalent to the well-known PD [13, 56] and AR decoding [43, 45], standardized as an instruction-guided

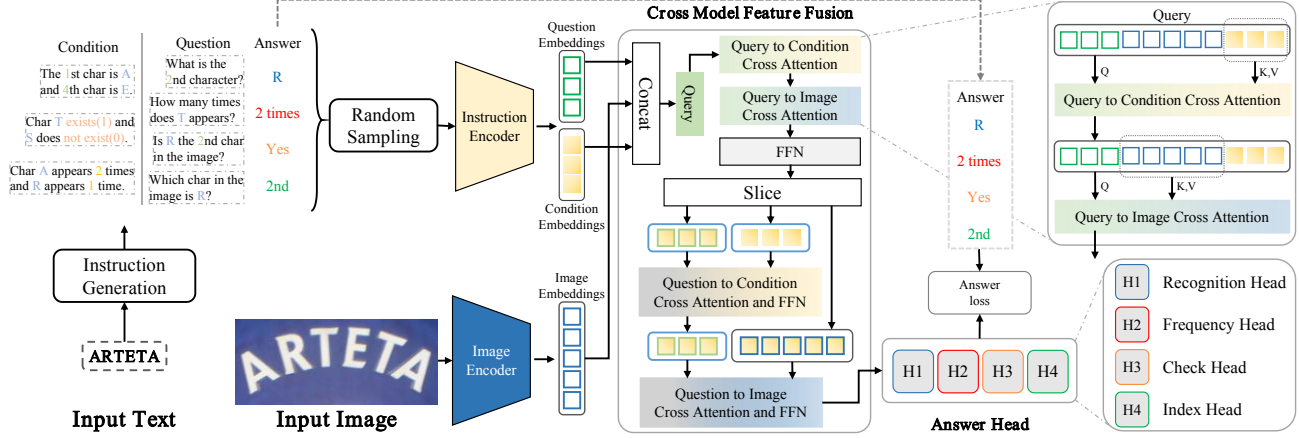


Figure 2. Overview of Instruction-Guided Scene Text Recognition.

manner. The third is a re-identification task, which double-checks the character at a specified position for possible error correction. The last one illustrates extrapolating recognition, which differs from AR decoding in that they are substrings-based recognition, i.e., starting from an arbitrary position and without positioning information.

For instruction sampling, one practical issue is that the answer might already be covered by the condition if no sampling strategy is employed. To avoid this answer leaking, for each text image, a certain number of elements are randomly selected from the three sets of attributes mentioned in *condition*, i.e., determine the conditions at first, and leave the rest elements for question-answer pair generation. Then for each question, we exhaustively enumerate all possible variables and generate question-answer pairs accordingly. This process is repeated K times to generating rich and diverse instructions for each text image. All of them are utilized for model training. Note that the instructions are sampled online during the training, and we do not store them due to their large quantity.

3.3. IGTR Architecture

Instruction and image encoders. Fig. 3 shows the instruction encoder in detail. It consists of four components each responsible for extracting embeddings for a different kind of information. Conditions and questions are formatted in either unitary or pairwise forms. The unitary ones include character, frequency, and position in *question*, which are directly mapped to their respective embeddings using the corresponding encoder modules. The pairwise ones for *condition* include character-existence, character-frequency and character-position, whose embeddings are obtained by summing up their constituent embeddings. On the other hand for the pairwise compound *question*, the embeddings are composed of its unitary question embeddings summed up with the constraint embeddings. On the image side, we uti-

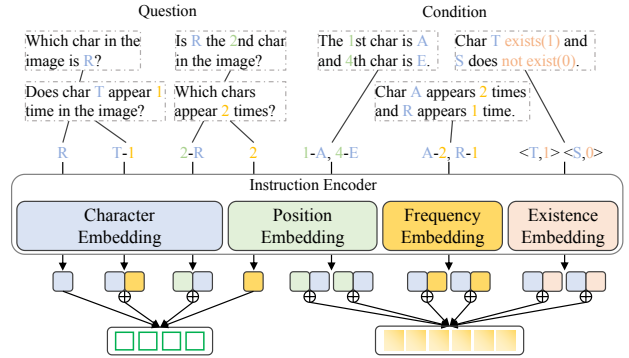


Figure 3. Overview of Instruction Encoder.

lize SVTR-B backbone [11] (with the rectification module and CTC decoder removed) as the encoder. The extracted visual features are flattened as the image embeddings.

Cross-modal feature fusion. We devise a dedicated cross-modal feature fusion (CMFF) module to fuse condition, question and image embeddings. First, the three embeddings are concatenated to form a *Query*. Four cross-attention stages are developed for feature fusion, the first two respective using the condition and image embeddings as *Key* and *Value*. Therefore the query absorbs desired information from both condition and image sides, being understood as reading the known attributes and seeing the image content. Then, the query feature is sliced back to condition, question, and image embeddings of original shapes. In the following, the question embedding is employed as the *Query*, and question-to-condition and question-to-image cross-attentions are successively conducted, from which the question extracts finer condition and image features to obtain answer-related cross-modal question embeddings.

Answer head. With the question embeddings, we construct a multi-task answer head to perform character attribute pre-

Question (with all conditions)	PD	AR	Next
(a): recognition task	80.57	81.27	80.79
(b): (a) + statistic inference task	81.22	82.21	81.98
(c): (b) + character search task	81.94	83.53	82.18
(d): (c) + sub-string matching task	82.37	84.02	83.21
Condition (with all questions)	PD	AR	Next
(e): w/o condition	79.02	-	-
(f): (e) + cond-1	79.82	-	-
(g): (f) + cond-2	80.90	-	-
(h): (g) + cond-3	81.35	82.93	-
(i): (h) + cond-4	82.23	83.97	83.25
K (with all conditions and questions)	PD	AR	Next
2	80.53	82.41	81.96
4	81.68	83.39	82.85
6	81.92	83.87	83.33
(j): ((d)+constraint, (i)+cond-5, K=8)	82.51	84.86	83.78

Table 3. Ablations on instruction variants.

diction and recognition. The answer head is composed of four classification sub-heads, each corresponding to a specified kind of answer. Specifically, the *recognition* head, *check* head, *frequency* head, and *index* head are responsible for instructions whose answer is the character, check status (*Yes* or *No*), character frequency, character position index, respectively. During model training, prediction results of the four sub-heads are compared with the answer label to calculate loss, where cross-entropy loss is employed. The four kinds of losses are summed up as the overall loss to optimize the parameters of IGTR end to end.

4. Experiments

4.1. Datasets and Implementation Details

We evaluate IGTR on both English and Chinese datasets. For English our models are trained on two widely used synthetic scene text datasets, i.e., MJSynth (MJ) [20, 48] and SynthText (ST) [17]. Then the models are tested on: (1) six regular and irregular text benchmarks, i.e., ICDAR 2013 (IC13) [24], Street View Text (SVT) [50], IIIT5K-Words (IIIT) [38], ICDAR 2015 (IC15) [23], Street View Text-Perspective (SVTP) [39] and CUTE80 (CUTE) [1]. For IC13 and IC15, we use the versions with 857 and 1,811 images, respectively. We abbreviate the six benchmarks as common benchmarks. (2) the recently built Union14M-L benchmark. It contains over 3.2 million training images and over 0.4 million test images. All are real-world images with both complexity and versatility [22]. The test set includes seven challenging subsets such as curve, multi-oriented, artistic, etc. For Chinese, we use Chinese text recognition (CTR) dataset [6], a benchmark containing four challenging subsets: Scene, Web, Document, and Writing. For each subset, we train the model on the whole training

Model	PD	AR	Next
Full Model	82.51	84.86	83.78
(a): w/o Query to Condition	81.75	82.41	82.13
(b): w/o Query to Image	81.85	82.35	82.02
(c): (a) + (b)	80.85	81.23	80.83
(d): w/o Question to Condition	81.96	82.22	82.01
(e): w/o Question to Image	81.34	83.21	82.88
(f): (d) + (e)	80.93	82.01	81.25

Table 4. Ablations on CMFF components.

set and use its validation subset to determine the best model, which is then assessed on the test subset.

We use AdamW optimizer [34] with a weight decay of 0.05 for training. For English models, All text images are resized to a maximum pixel count of 32×128 [3, 14, 61] maintaining aspect ratio. The learning rate (LR) is set to 5×10^{-4} and batchsize is set to 1024. One cycle LR scheduler [47] with 1.5 epochs linear warm-up is used in all the 20 epochs. The same as [3, 11, 14, 22], data augmentation like rotation, perspective distortion, motion blur and gaussian noise, are randomly performed during training. The alphabet includes all case-insensitive alphanumeric. For Chinese models, all text instances are resized to 32×256 and data augmentation is not performed following [57]. The LR is set to 5×10^{-4} and batchsize is set to 512. One cycle LR scheduler with 3 epochs linear warm-up is used in all 100 epochs. Word accuracy is used as the evaluation metric. The size of the character set C is set to 37 for English and 6625 for Chinese [28]. The maximum prediction length L is set to 25 for both. All models are trained with mixed-precision on 2 Tesla A100 GPUs.

4.2. Ablations

We conduct ablation studies on the Union14M-L benchmark to validate different instruction variants, CMFF components, and model scalability as follows.

Instruction variants. We conduct experiments to validate the effectiveness of the triplet-designed instruction and its components. The results in Tab. 3 include IGTR-PD (PD), IGTR-AR (AR) and extrapolating recognition (Next). In (a), only recognition instructions guide the IGTR model training. In subsequent variations denoted by (b), (c), (d), and (j), we add different task types progressively. The outcomes reveal that each attribute prediction task contributes positively, supporting the idea that understanding diverse character attributes aids in recognition. Comparing the use of full instructions in (j) to (a), PD improved by +1.94%, AR by +3.59%, and Next by +2.99%, indicating that AR and Next are more sensitive to the diversity of question types, due to their reliance on already mastered information. On the other hand, we perform (e) without condition (*cond*), and then progressively add a condition mode

Epoch	20	40	60	Model Size	23M	40M
Vanilla PD	76.14	76.89	77.05	Vanilla PD	76.14	76.23
IGTR-PD	82.51	84.06	85.29	IGTR-PD	82.51	83.60

Table 5. Ablations on training data volume and model size.

Question	Common	Union14M-L
Constraint statistics	94.43	80.22
Check character search	95.31	82.33

Table 6. Zero-Shot prediction results of using different questions.

Model	$Rare_{1-10}$	$Rare_{11-30}$	$Rare_{31-50}$	Avg
IGTR-PD	63.88	84.93	88.79	72.25
IGTR-PD-TS	67.47	86.61	89.86	75.05

Table 7. Rarely appeared character results on Chinese Text Benchmarks [6].

in (f)-(j). IGTR acquires AR and Next decoding capabilities only when *cond-3* and *cond-4* are successively added. The results show that conditions not only enhance accuracy but also realize different decoding methods conveniently by adapting the instruction. Additionally, by increasing K , the number of sampling times, the accuracy steadily improved, providing intuitive confirmation of the importance of instruction richness and diversity.

CFMM components. As shown in Fig. 2, CFMM incorporates four cross-attention stages for inter-modal interaction. We devise several variants by removing different sets of stages, and the results are presented in Tab. 4. Removing any type of cross-attention results in a decrease in accuracy. Notably, the most significant average drop of 2.81% occurs when both query-to-condition and query-to-image cross-attention stages are removed, emphasizing the necessity of sufficient feature interaction and fusion before making predictions. In addition, the conditions for AR and Next are derived from preceding decoding results while for PD is set to None. It is anticipated that query-to-condition and query-to-image have a more pronounced impact on AR and Next, while PD remains relatively unaffected. The analysis explains a consistent accuracy degradation of 3.63% for AR and 2.95% for Next. Interestingly, PD also experiences a 1.66% decrease, albeit less severe than AR and Next. This could be attributed to that the query-to-condition and query-to-image cross-attention stages have encoded ample instruction patterns during training, which are beneficial to the three recognition schemes.

Scalability of IGTR. We conduct ablations on training data volume and model size, where IGTR-PD and vanilla PD (without using instructions) are selected. The results are presented in the left half of Tab. 5, where different train-

Char	菜	x	+	太	干	已
	8/5(菜)	8/4(x)	22/14(十)	20/12(大)	13/11(千)	10/6(己)
Char	入	土	域	日	筒	z
	12/8(人)	4/2(士)	6/3(城)	6/5(日)	6/4(筒)	12/5(2)
Char	金	全	内	于	天	凤
	26/15(全)	16/10(金)	15/8(肉)	13/8(子)	12/5(大)	12/9(凤)
Char	v	东	i	字	自	着
	22/15(y)	7/4(乐)	106/86(l)	9/4(字)	8/5(白)	8/6(看)

Table 8. Similar morphological characters and mis-recognitions on Chinese Text Benchmarks [6]. Take "菜-菜" and 8/5 as the example. It means that without considering TS, "菜" has been recognized as "菜" for 8 times, and the number is reduced to 5 when TS is employed.

ing epochs are considered. We observe a notable accuracy gain of 2.78% when increasing epochs from 20 to 60 for IGTR-PD. This improvement is accompanied by the expansion of data volume, as IGTR-PD samples instructions individually at each epoch. Since different instructions may be selected, the trained model benefits from both more training samples and epochs. In contrast, the improvement of vanilla PD is 0.91%, solely from more training epochs. The significant improvement gap (2.78% v.s. 0.91%) implies that IGTR-PD largely benefits from the training data volume. Furthermore, the right half of Tab. 5 also shows that the accuracy increases with model size. The 23M and 40M models correspond to using SVTR-B and SVTR-L [11] as the image encoder, with the remaining architecture keeping the same. We observe a similar large improvement gap (1.09% v.s. 0.09%) between the two methods, suggesting that instruction-guided learning can evoke a superior modeling capability for a larger model.

4.3. Zero-shot Prediction

Benefiting from the flexibility of the proposed instruction-guided scheme, text recognition can also be achieved by adjusting character attribute prediction instructions alone, devoid of recognition instructions. This corresponds to an approach commonly denoted as zero-shot recognition [25, 30, 32, 42]. Consequently, we conduct validation experiments to assess the zero-shot capability of IGTR (IGTR-Zero), which is trained exclusively with attribute prediction instructions.

With the IGTR-Zero, we test two schemes, i.e., using question *constraint statistics* or *check character search* (see Tab. 1) to infer the text. The former one, by combining with another pre-learned *pre-task identification* question that tells the first character, enables stepwise inference of the second (by setting the second variable in the question as 2), third, and subsequent characters, thus recognizing the

Method	Common Benchmarks								Union14M-L Benchmarks								Parameters ($\times 10^6$)
	IC13	SVT	IIIT	IC15	SVTP	CUTE	Avg	Curve	Multi-Oriented	Artistic	Contextless	Salient	Multi-Words	General	Avg		
CTC	CRNN [44]	91.1	81.6	82.9	69.4	70.0	65.5	76.75	7.5	0.9	20.7	25.6	13.9	25.6	32.0	18.03	8.3
	SVTR-B [11]	97.1	91.5	96.0	85.2	89.9	91.7	91.90	69.8	37.7	47.9	61.4	66.8	44.8	61.0	55.63	24.6
AR	ASTER [45]	90.8	90.0	93.3	74.7	80.2	80.9	84.98	34.0	10.2	27.7	33.0	48.2	27.6	39.8	31.50	27.2
	NRTR [43]	95.8	91.5	90.1	79.4	86.6	80.9	87.38	31.7	4.4	36.6	37.3	30.6	54.9	48.0	34.79	31.7
	SAR [29]	91.0	84.5	91.5	69.2	76.4	83.5	82.68	44.3	7.7	42.6	44.2	44.0	51.2	50.5	40.64	57.7
	RoScanner [58]	94.8	88.1	95.3	77.1	79.5	90.3	87.52	43.6	7.9	41.2	42.6	44.9	46.9	39.5	38.09	48.0
	PARSeq [3]	97.0	93.6	97.0	86.5	88.9	92.2	92.53	63.9	16.7	52.5	54.3	68.2	55.9	56.9	52.62	23.8
	CDisNet [61]	97.4	93.5	96.4	86.0	88.7	93.4	92.57	69.3	24.4	49.8	55.6	72.8	64.3	58.5	56.38	65.5
PD	SRN [56]	95.5	91.5	94.8	82.7	85.1	87.8	89.57	63.4	25.3	34.1	28.7	56.5	26.7	46.3	40.14	54.7
	VisionLAN [53]	95.7	91.7	95.8	83.7	86.0	88.5	90.23	57.7	14.2	47.8	48.0	64.0	47.9	52.1	47.39	32.8
	ABINet [14]	97.4	93.5	96.2	86.0	89.3	89.2	91.93	59.5	12.7	43.3	38.3	62.0	50.8	55.6	46.03	36.7
	GTR [18]	96.8	94.1	95.8	84.6	87.9	92.3	91.92	62.3	13.9	50.0	45.1	67.1	53.4	58.5	50.07	42.1
	LPV-B [59]	97.6	94.6	97.3	87.5	90.9	94.8	93.78	68.3	21.0	59.6	65.1	76.2	63.6	62.0	59.40	35.1
Ours	IGTR-PD	97.6	95.2	97.6	88.4	91.6	95.5	94.30	76.9	30.6	59.1	63.3	77.8	62.5	66.7	62.40	24.1
	IGTR-AR	98.6	95.7	98.2	88.4	92.4	95.5	94.78	78.4	31.9	61.3	66.5	80.2	69.3	67.9	65.07	24.1

Table 9. Results on English benchmarks tested against existing models when trained on synthetic datasets.

Method	Common Benchmarks								Union14M-L Benchmarks								Parameters ($\times 10^6$)
	IC13	SVT	IIIT	IC15	SVTP	CUTE	Avg	Curve	Multi-Oriented	Artistic	Contextless	Salient	Multi-Words	General	Avg		
CTC	CRNN [44]	91.8	83.8	90.8	71.8	70.4	80.9	81.58	19.4	4.5	34.2	44.0	16.7	35.7	60.4	30.70	8.3
	SVTR-B [11]	97.5	96.4	97.8	89.3	91.0	96.2	94.72	85.4	87.4	68.9	79.5	84.3	79.1	81.8	80.91	24.6
AR	ASTER [45]	92.6	88.9	94.3	77.7	80.5	86.5	86.75	38.4	13.0	41.8	52.9	31.9	49.8	66.7	42.07	27.2
	NRTR [43]	96.9	94.0	96.2	80.9	84.8	92.0	90.80	49.3	40.6	54.3	69.6	42.9	75.5	75.2	58.20	31.7
	SAR [29]	96.0	92.4	96.6	82.0	85.7	92.7	90.90	68.9	56.9	60.6	73.3	60.1	74.6	76.0	67.20	57.7
	RoScanner [58]	95.7	92.4	96.8	86.4	83.9	93.8	91.50	66.2	54.2	61.4	72.7	60.1	74.2	75.7	66.36	48.0
	MAERec [22]	97.6	96.8	98.0	87.1	93.2	97.9	95.10	81.4	71.4	72.0	82.0	78.5	82.4	82.5	78.60	35.7
PD	SRN [56]	94.7	89.5	95.5	79.1	83.9	91.3	89.00	49.7	20.0	50.7	61.0	43.9	51.5	62.7	48.50	54.7
	VisionLAN [53]	95.1	91.3	96.3	83.6	85.4	92.4	90.68	70.7	57.2	56.7	63.8	67.6	47.3	74.2	62.50	32.8
	ABINet [14]	97.2	95.7	97.2	87.6	92.1	94.4	94.03	75.0	61.5	65.3	71.1	72.9	59.1	79.4	69.19	36.7
Ours	IGTR-PD	97.7	97.7	98.3	89.8	93.7	97.9	95.86	88.1	89.9	74.2	80.3	82.8	79.2	83.0	82.51	24.1
	IGTR-AR	98.1	98.4	98.7	90.5	94.9	98.3	96.48	90.4	91.2	77.0	82.4	84.7	84.0	84.4	84.86	24.1
	IGTR-PD-PT	98.6	98.0	99.1	91.7	96.8	99.0	97.20	92.4	92.1	80.7	83.6	87.7	86.9	85.0	86.92	24.1
	IGTR-AR-PT	98.8	98.3	99.2	92.0	96.8	99.0	97.34	93.0	92.9	81.3	83.4	88.6	88.7	85.6	87.65	24.1

Table 10. Results on English benchmarks tested against existing models when trained on real-world Union14M-L dataset.

whole text. The results are presented in Tab. 6. However, this inference chain is relatively complex such that the model only achieves moderate success on more challenging datasets (80.22% on Union14M-L). Nevertheless, it still excels most existing models in Tab. 10. The latter one, by traversing all characters with all positions, presents a more straightforward and less question-dependent way to determine the text, thus reaching an accuracy of 82.33%. It outperforms SVTR-B, the previous best, by 1.42%. The result again demonstrates the superiority of IGTR-Zero.

4.4. Dealing with Typical Challenges

Rarely appeared and morphologically similar character recognition are two typical challenges in STR, especially for languages with a large number of character categories,

e.g., Chinese. Owing to the flexibility of the instruction-guided scheme, we devise an elegant scheme to alleviate the two challenges by adjusting the bias of instruction sampling. Specifically, given a rarely appeared character c_i , we increase the sampling probability of instructions containing c_i , e.g., *Is c_i the j -th character in the image?*. Similarly, for morphologically similar character pairs (“大-太”, z-2, 1-1, etc.), we increase the sampling probability of questions such as *Is the i -th character “太”?* when the answer is “大”. By doing so, rarely appeared characters and morphologically similar character pairs have been emphasized during the training, and thus can be better identified.

We term the adjustments above as targeted strengthening (TS) and devise a scheme termed IGTR-PD-TS accordingly. Results on the CTR dataset are presented in Tab. 7 and Tab.

Method	Scene	Web	Docu- ment	Hand- writing	Avg	Params ($\times 10^6$)
CRNN [44]	53.4	57.0	96.6	50.8	64.45	12.4
ASTER [45]	61.3	51.7	96.2	37.0	61.55	27.2
MORAN [36]	54.6	31.5	86.1	16.2	47.10	28.5
SAR [29]	59.7	58.0	95.7	36.5	62.48	27.8
SEED [40]	44.7	28.1	91.4	21.0	46.30	36.1
MASTER [35]	62.8	52.1	84.4	26.9	56.55	62.8
ABINet [14]	66.6	63.2	98.2	53.1	70.28	53.1
TransOCR [5]	71.3	64.8	97.1	53.0	71.55	83.9
SVTR-B [11]	71.7	73.8	98.2	52.2	73.98	26.3
CCR-CLIP [57]	71.3	69.2	98.3	60.3	74.78	62.0
IGTR-PD	73.1	74.8	98.6	52.5	74.75	29.2
IGTR-AR	75.1	76.4	98.7	55.3	76.37	29.2
IGTR-PD-TS	73.5	75.9	98.7	54.5	75.65	29.2
IGTR-AR-TS	75.6	77.0	98.8	57.3	77.17	29.2
IGTR-PD-Aug	79.5	80.0	99.4	58.9	79.45	29.2
IGTR-AR-Aug	82.0	81.7	99.5	63.8	81.74	29.2

Table 11. Results on CTR dataset tested against existing models.

8. In Tab. 7, rarely appeared characters are grouped into three classes according to their occurrences. Compared to vanilla IGTR-PD, the accuracy gaps are 3.59%, 1.68%, and 1.07% for characters appearing 1 to 10, 11 to 30, and 31 to 50 times, respectively. Larger gains are observed in severely rare characters. Meanwhile in Tab. 8, each pair gives two values, e.g., 8/5 for the "菜-菜" pair. It means that without considering TS, "菜" has been classified as "菜" 8 times, and when TS is employed, the times are reduced from 8 to 5. It is seen that recognition errors occurred between morphologically similar characters are largely reduced. Both experiments convincingly verify the flexibility of IGTR and its potential in addressing typical STR challenges.

4.5. Comparison with State-of-the-Art

We compare IGTR with previous models on both Common and Union14M-L benchmarks. The results trained based on synthetic and Union14M-L datasets are presented in Tab. 9 and Tab. 10, respectively. Meanwhile, we also train IGTR in a two-step manner: first pre-training with attribute prediction instructions on synthetic datasets, and then fine-tuning with recognition instructions on the Union14M-L benchmark. The obtained models are marked with a suffix PT.

As can be seen, IGTR-AR and IGTR-AR-PT respectively rank the top among 12 of the 13, and 11 of the 13 subsets when inspected individually. IGTR-AR outperforms LPV-B [59], the best previous model in Tab. 9, by 1.0% and 5.67% in average on Common and Union14M-L benchmarks. While for IGTR-AR-PT, the accuracy gap to the best previous model in Tab. 10 is prominent 2.24% and 6.74%, respectively. The results convincingly demonstrate the superiority of our instruction-guided learning. Meanwhile, by adopting the PT training strategy, performance gains ranging from 2.79%-4.41% on Union14M-L are observed for

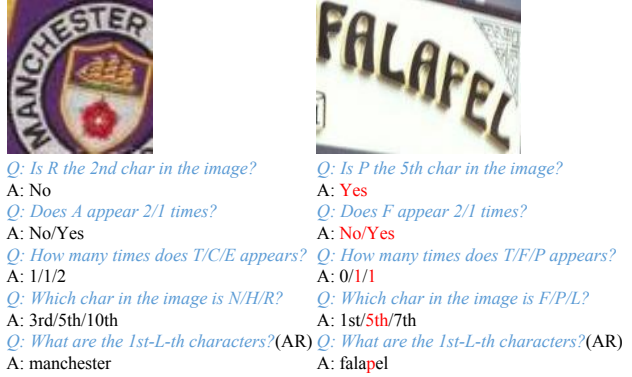


Figure 4. Success and failure cases of IGTR, where the wrong answers are marked in red.

both PD and AR-based methods. It suggests that IGTR benefits from the comprehension-first and prediction-next pipeline. Note that IGTR is even smaller than SVTR-B in model size. This is because we only use the SVTR-B backbone, and CFMM and the answer head are both lightweight. Regarding the inference speed, IGTR-PD and IGTR-AR attain 255 FPS and 95 FPS tested on one GTX 1080Ti GPU, respectively, which are also highly competitive compared to existing models.

In Tab. 11, we also give the comparisons in the CTR benchmark. IGTR still outperforms existing models by clear margins, especially for those employing targeted strengthening (TS). Additionally, we implement data augmentation to mitigate overfitting in IGTR (IGTR-*-Aug), resulting in a further enhancement in accuracy across all subsets. The results clearly validate the great cross-language generalization ability of IGTR.

We present two success and failure cases in Fig. 4. The left one correctly answers the questions and understands the text image, thus inferring the text properly. Note that this ability is acquired by rich and diverse cross-modal interactions rather than language models solely [13]. While for the right one, since all attribute inferences have made the same mistake, resulting in a failed prediction. Both cases illustrate the instruction-guided characteristic of IGTR.

5. Conclusion

In this paper, we present IGTR, a novel instruction-guided multi-modal STR model. We construct rich and diverse instruction triplets as training data, and develop an architecture with dedicated instruction encoder, CFMM module, and answer head to effectively process the instructions. Consequently, IGTR acquires the ability to comprehend text image and accurately predicts the text. Extensive experiments on public benchmarks demonstrate the effectiveness of IGTR. IGTR not only excels existing models by clear margins, but also the unique learning paradigm enables a set

of new recognition schemes via adjusting the instructions. For example, owing to comprehending the text image, IGTR recognizes text well although not trained directly on recognition instructions. Moreover, IGTR effectively recognizes rarely appeared and morphologically similar characters, which are typical challenges for existing models. In addition, our instruction-guided scheme could be integrated with large multi-modal models [8, 10, 31, 55, 62] for further improvement, which constitute our future work.

References

- [1] R. Anhar, S. Palaiahnakote, C. S. Chan, and C. L. Tan. A robust arbitrary text detection system for natural scene images. *Expert Syst. Appl.*, pages 8027–8048, 2014. [5](#)
- [2] S. Antol, A. Agrawal, J. Lu, M. Mitchell, D. Batra, C. Zitnick, and D. Parikh. Vqa: Visual question answering. In *ICCV*, pages 2425–2433, 2015. [3](#)
- [3] D. Bautista and R.I. Atienza. Scene text recognition with permuted autoregressive sequence models. In *ECCV*, pages 178–196, 2022. [1](#), [3](#), [5](#), [7](#), [4](#)
- [4] Maurits Bleeker and Maarten de Rijke. Bidirectional scene text recognition with a single decoder. *arXiv preprint arXiv:1912.03656*, 2019. [3](#)
- [5] J. Chen, B. Li, and X. Xue. Scene text telescope: Text-focused scene image super-resolution. In *CVPR*, pages 12021–12030, 2021. [8](#)
- [6] J. Chen, H. Yu, J. Ma, M. Guan, X. Xu, X. Wang, S. Qu, B. Li, and X. Xue. Benchmarking chinese text recognition: Datasets, baselines, and an empirical study. *arXiv:2112.15093*, 2021. [5](#), [6](#)
- [7] X. Chen, L. Jin, Y. Zhu, C. Luo, and T. Wang. Text recognition in the wild: A survey. *ACM Computing Surveys (CSUR)*, 54(2):1–35, 2021. [3](#)
- [8] W. Dai, J. Li, D. Li, A. Tiong, J. Zhao, W. Wang, B. Li, P. Fung, and S. Hoi. Instructblip: Towards general-purpose vision-language models with instruction tuning, 2023. [9](#)
- [9] S. Deshmukh, B. Elizalde, R. Singh, and H. Wang. Pengi: An audio language model for audio tasks, 2023. [3](#)
- [10] D. Driess, F. Xia, M. Sajjadi, C. Lynch, A. Chowdhery, B. Ichter, A. Wahid, J. Tompson, Q. Vuong, T. Yu, W. Huang, Y. Chebotar, P. Sermanet, D. Duckworth, S. Levine, V. Vanhoucke, K. Hausman, M. Toussaint, K. Greff, A. Zeng, I. Mordatch, and P. Florence. Palm-e: An embodied multi-modal language model, 2023. [9](#)
- [11] Y. Du, Z. Chen, C. Jia, X. Yin, T. Zheng, C. Li, Y. Du, and Y. Jiang. Svtr: Scene text recognition with a single visual model. In *IJCAI*, pages 884–890, 2022. [3](#), [4](#), [5](#), [6](#), [7](#), [8](#), [1](#)
- [12] Y. Du, Z. Chen, C. Jia, X. Yin, C. Li, Y. Du, and Y. Jiang. Context perception parallel decoder for scene text recognition, 2023. [3](#)
- [13] S. Fang, H. Xie, Y. Wang, Z. Mao, and Y. Zhang. Read like humans: Autonomous, bidirectional and iterative language modeling for scene text recognition. In *CVPR*, pages 7098–7107, 2021. [1](#), [3](#), [8](#)
- [14] S. Fang, Z. Mao, H. Xie, Y. Wang, C. Yan, and Y. Zhang. Abinet++: Autonomous, bidirectional and iterative language modeling for scene text spotting. *IEEE Trans. Pattern Anal. Mach. Intell.*, 45(6):7123–7141, 2023. [5](#), [7](#), [8](#), [4](#)
- [15] R. Girshick, J. Donahue, T. Darrell, and J. Malik. Rich feature hierarchies for accurate object detection and semantic segmentation. In *CVPR*, pages 580–587, 2014. [1](#), [3](#)
- [16] A. Graves, S. Fernández, F. Gomez, and J. Schmidhuber. Connectionist temporal classification: Labelling unsegmented sequence data with recurrent neural networks. In *ICML*, page 369–376, 2006. [3](#)
- [17] A. Gupta, A. Vedaldi, and A. Zisserman. Synthetic data for text localisation in natural images. In *CVPR*, pages 2315–2324, 2016. [5](#)
- [18] Y. He, C. Chen, J. Zhang, J. Liu, F. He, C. Wang, and B. Du. Visual semantics allow for textual reasoning better in scene text recognition. In *AAAI*, pages 888–896, 2022. [7](#)
- [19] W. Hu, X. Cai, J. Hou, S. Yi, and Z. Lin. Gtc: Guided training of ctc towards efficient and accurate scene text recognition. In *AAAI*, pages 11005–11012, 2020. [3](#)
- [20] M. Jaderberg, K. Simonyan, A. Vedaldi, and A. Zisserman. Synthetic data and artificial neural networks for natural scene text recognition. In *NeurIPS Deep Learning Workshop*, 2014. [5](#)
- [21] C. Jia, Y. Yang, Y. Xia, Y. Chen, Z. Parekh, H. Pham, Q. Le, Y. Sung, Z. Li, and T. Duerig. Scaling up visual and vision-language representation learning with noisy text supervision. In *ICML*, pages 4904–4916. PMLR, 2021. [3](#)
- [22] Q. Jiang, J. Wang, D. Peng, C. Liu, and L. Jin. Revisiting scene text recognition: A data perspective. In *ICCV*, 2023. [5](#), [7](#), [4](#)
- [23] D. Karatzas, L. Gomez-Bigorda, A. Nicolaou, S. Ghosh, A. Bagdanov, M. Iwamura, J. Matas, L. Neumann, V. R. Chandrasekhar, S. Lu, F. Shafait, S. Uchida, and E. Valveny. Icdar 2015 competition on robust reading. In *ICDAR*, pages 1156–1160, 2015. [5](#)
- [24] D. KaratzasAU, F. ShafaitAU, S. UchidaAU, M. IwamuraAU, L. G. i. BigordaAU, S. R. MestreAU, J. MasAU, D. F. MotaAU, J. A. AlmazànAU, and L. P. de las Heras. Icdar 2013 robust reading competition. In *ICDAR*, pages 1484–1493, 2013. [5](#)
- [25] A. Kirillov, E. Mintun, N. Ravi, H. Mao, C. Rolland, L. Gustafson, T. Xiao, S. Whitehead, A. Berg, W. Lo, P. Dollar, and R. Girshick. Segment anything. In *ICCV*, pages 4015–4026, 2023. [1](#), [3](#), [6](#)
- [26] C. Lai, Z. Lu, L. Cao, and R. Pang. Instruction-following speech recognition, 2023. [3](#)
- [27] J. Lee, S. Park, J. Baek, S. Oh, S. Kim, and H. Lee. On recognizing texts of arbitrary shapes with 2d self-attention. In *CVPR Workshops*, pages 546–547, 2020. [3](#)
- [28] C. Li, W. Liu, R. Guo, X. Yin, K. Jiang, Y. Du, Y. Du, L. Zhu, B. Lai, X. Hu, D. Yu, and Y. Ma. Pp-ocrv3: More attempts for the improvement of ultra lightweight ocr system. *CoRR*, abs/2206.03001, 2022. [5](#)
- [29] H. Li, P. Wang, C. Shen, and G. Zhang. Show, attend and read: A simple and strong baseline for irregular text recognition. In *AAAI*, pages 8610–8617, 2019. [3](#), [7](#), [8](#)
- [30] L. Li, P. Zhang, H. Zhang, J. Yang, C. Li, Y. Zhong, L. Wang, L. Yuan, L. Zhang, J. Hwang, et al. Grounded language-

- image pre-training. In *CVPR*, pages 10965–10975, 2022. 1, 3, 6
- [31] Haotian Liu, Chunyuan Li, Qingyang Wu, and Yong Jae Lee. Visual instruction tuning, 2023. 9
- [32] S. Liu, Z. Zeng, T. Ren, F. Li, H. Zhang, J. Yang, C. Li, J. Yang, H. Su, J. Zhu, et al. Grounding dino: Marrying dino with grounded pre-training for open-set object detection. *arXiv preprint arXiv:2303.05499*, 2023. 1, 3, 6
- [33] J. Long, E. Shelhamer, and T. Darrell. Fully convolutional networks for semantic segmentation. In *CVPR*, pages 3431–3440, 2015. 1, 3
- [34] I. Loshchilov and F. Hutter. Decoupled weight decay regularization. In *ICLR*, 2019. 5
- [35] N. Lu, W. Yu, X. Qi, Y. Chen, P. Gong, R. Xiao, and X. Bai. Master: Multi-aspect non-local network for scene text recognition. *Pattern Recognit.*, page 107980, 2021. 8
- [36] C. Luo, L. Jin, and Z. Sun. Moran: A multi-object rectified attention network for scene text recognition. *Pattern Recognit.*, pages 109–118, 2019. 8
- [37] G. Lv, X. Jiang, Y. Sun, W. Ni, and F. Nian. Vqa-clpr: Turning a visual question answering model into a chinese license plate recognizer. In *ICIG*, pages 348–359, 2023. 3
- [38] A. Mishra, A. Karteek, and C. V. Jawahar. Scene text recognition using higher order language priors. In *BMVC*, 2012. 5
- [39] T. Q. Phan, P. Shivakumara, S. Tian, and C. L. Tan. Recognizing text with perspective distortion in natural scenes. In *CVPR*, pages 569–576, 2013. 5
- [40] Z. Qiao, Y. Zhou, D. Yang, Y. Zhou, and W. Wang. Seed: Semantics enhanced encoder-decoder framework for scene text recognition. In *CVPR*, pages 13525–13534, 2020. 8
- [41] Z. Qiao, Y. Zhou, J. Wei, W. Wang, Y. Zhang, N. Jiang, H. Wang, and W. Wang. Pimnet: a parallel, iterative and mimicking network for scene text recognition. In *ACM MM*, pages 2046–2055, 2021. 3
- [42] A. Radford, J. Kim, C. Hallacy, A. Ramesh, G. Goh, S. Agarwal, G. Sastry, A. Askell, P. Mishkin, J. Clark, G. Krueger, and I. Sutskever. Learning transferable visual models from natural language supervision. In *ICML*, pages 8748–8763. PMLR, 2021. 3, 6
- [43] F. Sheng, Z. Chen, and B. Xu. Nrtr: A no-recurrence sequence-to-sequence model for scene text recognition. In *ICDAR*, pages 781–786, 2019. 1, 3, 7
- [44] B. Shi, X. Bai, and C. Yao. An end-to-end trainable neural network for image-based sequence recognition and its application to scene text recognition. *IEEE Trans. Pattern Anal. Mach. Intell.*, pages 2298–2304, 2017. 3, 7, 8
- [45] B. Shi, M. Yang, X. Wang, P. Lyu, C. Yao, and X. Bai. Aster: An attentional scene text recognizer with flexible rectification. *IEEE Trans. Pattern Anal. Mach. Intell.*, pages 2035–2048, 2019. 3, 7, 8, 4, 5
- [46] A. Vaswani, N. Shazeer, N. Parmar, J. Uszkoreit, L. Jones, A. Gomez, Ł. Kaiser, and I. Polosukhin. Attention is all you need. In *NIPS*, 2017. 3
- [47] I. Loshchilov and F. Hutter. SGDR: stochastic gradient descent with warm restarts. In *ICLR*, 2017. 5
- [48] M. Jaderberg, K. Simonyan, A. Vedaldi, and A. Zisserman. Reading text in the wild with convolutional neural networks. In *IJCV*, pages 1–20, 2015. 5
- [49] Z. Wan, M. He, H. Chen, X. Bai, and C. Yao. Textscanner: Reading characters in order for robust scene text recognition. In *AAAI*, pages 12120–12127, 2020. 3
- [50] K. Wang, B. Babenko, and S. Belongie. End-to-end scene text recognition. In *ICCV*, pages 1457–1464, 2011. 5
- [51] P. Wang, A. Yang, R. Men, J. Lin, S. Bai, Z. Li, J. Ma, C. Zhou, J. Zhou, and H. Yang. Ofa: Unifying architectures, tasks, and modalities through a simple sequence-to-sequence learning framework. In *ICML*, pages 23318–23340. PMLR, 2022. 3
- [52] X. Wang, X. Zhang, Y. Cao, W. Wang, C. Shen, and T. Huang. Seggpt: Towards segmenting everything in context. In *ICCV*, pages 1130–1140, 2023. 1, 3
- [53] Y. Wang, H. Xie, S. Fang, J. Wang, S. Zhu, and Y. Zhang. From two to one: A new scene text recognizer with visual language modeling network. In *ICCV*, pages 14194–14203, 2021. 1, 3, 7
- [54] L. Yang, D. Ergu, Y. Cai, F. Liu, and B. Ma. A review of natural scene text detection methods. *Procedia Computer Science*, 199:1458–1465, 2022. 3
- [55] Z. Yang, L. Li, K. Lin, J. Wang, C. Lin, Z. Liu, and L. Wang. The dawn of lmms: Preliminary explorations with gpt-4v(ision), 2023. 9
- [56] D. Yu, X. Li, C. Zhang, T. Liu, J. Han, J. Liu, and E. Ding. Towards accurate scene text recognition with semantic reasoning networks. In *CVPR*, pages 12113–12122, 2020. 3, 7
- [57] H. Yu, X. Wang, B. Li, and X. Xue. Chinese text recognition with a pre-trained clip-like model through image-ids aligning. In *ICCV*, 2023. 5, 8
- [58] X. Yue, Z. Kuang, C. Lin, H. Sun, and W. Zhang. Robustscanner: Dynamically enhancing positional clues for robust text recognition. In *ECCV*, pages 135–151, 2020. 3, 7
- [59] B. Zhang, H. Xie, Y. Wang, J. Xu, and Y. Zhang. Linguistic more: Taking a further step toward efficient and accurate scene text recognition. In *IJCAI*, pages 1704–1712, 2023. 3, 7, 8
- [60] D. Zhang, S. Li, X. Zhang, J. Zhan, P. Wang, Y. Zhou, and X. Qiu. Speechgpt: Empowering large language models with intrinsic cross-modal conversational abilities, 2023. 3
- [61] T. Zheng, Z. Chen, S. Fang, H. Xie, and Y. Jiang. Cdistnet: Perceiving multi-domain character distance for robust text recognition. *International Journal of Computer Vision*, pages 1–19, 2023. 1, 3, 5, 7
- [62] D. Zhu, J. Chen, X. Shen, X. Li, and M. Elhoseiny. Minigtpt-4: Enhancing vision-language understanding with advanced large language models, 2023. 9

Instruction-Guided Scene Text Recognition

Supplementary Material

6. More Details of IGTR

6.1. The Details of IGTR pipeline

Algorithm 1 shows the pipeline of IGTR, primarily encompassing the instruction generation and forward process of the model. `GenInstruction` implements the instruction generation and sampling described in section 3.1. `GenCfCostrnt` generates the required condition-frequency pairs of the three constraint instructions by means of a constraint parameter. `GenQAbYTask` generates all available question-answer pairs with the attributes.

Taking *ARTETA* as an example, firstly, character attributes including character-existence (*ce*), character-frequency (*cf*) and position-character (*pc*) are generated. They are $[\langle A, 1 \rangle, \langle B, 0 \rangle, \dots, \langle E, 1 \rangle, \langle F, 0 \rangle, \dots, \langle R, 1 \rangle, \langle S, 0 \rangle, \langle T, 1 \rangle, \dots]$, $[A-2, E-1, R-1, T-2]$ and $[1-A, 2-R, 3-T, 4-E, 5-T, 6-A]$, respectively. Secondly, each attribute set is randomly divided into two subsets, one for creating conditions and the other for generating question-answer pairs. Assuming that the three condition subsets are $[\langle E, 1 \rangle, \langle R, 1 \rangle, \langle S, 0 \rangle]$, $[E-1, T-2]$ and $[1-A, 3-T, 6-A]$, respectively. This means that *cond-1* states “The characters *E* and *R* exist in the image, but *S* does not exist”; *cond-2* states “The character *T* appears twice and *E* appears once in the image”; and *cond-3* states “The 1-st character in the image is *A*, the 3-rd character is *T* and the 6-th character is *A*”. Taking *cond-3* as an example, the rest subset is $[2-R, 4-E, 5-T]$. Thus, the available questions are “Which character in the image is *R/E/T*?”, the answers are “The 2-nd/4-th/5-th one”, and other question-answer pairs can be generated like this. The question-answer pairs are classified as four types according to the answers (see the rightmost column in Tab. 1). Finally, they are split into two parts: *Ques* and *Ans*. *Ques* is fed into the instruction encoder along with *Cond* (condition). *Ans* is used as a label for calculating the loss. `GenSubString` randomly generates several sub-strings which are used to generate *cond-4*.

For a text image instance, the amount of generated instructions would be substantial. For example, an instruction set with quantity of $\sum_{p=1}^L (L-p) \frac{L!}{p!(L-p)!}$ can be generated using *cond-3*, and *cond-2* is also approximately the same. Therefore, although performing the pipeline only *K* times, a diverse and comprehensive range of instructions is generated, ensuring IGTR’s sufficient training.

6.2. The Details of IGTR Architecture

Image Encoder



Left: Instructions of constraint statistics task

Right: Instructions of check character search task

<i>Q: What are the first and last characters?</i>	<i>Q: What are the first and last characters?</i>
A: A/A	A: A/A
<i>Q: How many times does A/B/.../E/.../R/S/T/... appears in the first 2 characters?</i>	<i>Q: Is A/B/.../E/.../R/S/T/... the 2-nd character in the image?</i>
A: 1/0/.../0/.../1/0/0/...	A: No/No/.../No/.../Yes/No/No/...
Inferring 2-nd character is R	Inferring 2-nd character is R
<i>Q: How many times does A/B/.../E/.../R/S/T/... appears in the first 3 characters?</i>	<i>Q: Is A/B/.../E/.../R/S/T/... the 3-rd character in the image?</i>
A: 1/0/.../0/.../1/0/1/...	A: No/No/.../No/.../No/No/Yes/...
Inferring 3-rd character is T	Inferring 3-rd character is T
<i>Q: How many times does A/B/.../E/.../R/S/T/... appears in the first 4 characters?</i>	<i>Q: Is A/B/.../E/.../R/S/T/... the 4-th character in the image?</i>
A: 1/0/.../1/1/.../1/0/1/...	A: No/No/.../Yes/.../No/No/No/...
Inferring 4-th character is E	Inferring 4-th character is E
<i>Q: How many times does A/B/.../E/.../R/S/T/... appears in the first 5 characters?</i>	<i>Q: Is A/B/.../E/.../R/S/T/... the 5-th character in the image?</i>
A: 1/0/.../1/1/.../1/0/2/...	A: No/No/.../No/.../No/No/Yes/...
Inferring 5-th character is T	Inferring 5-th character is T
End: The text is arteta.	End: The text is arteta.

Figure 5. Illustration of using the two instructions described in Sec. 4.3 for zero-shot text inference.

Given a text image of size $H \times W \times 3$, the visual features $F_v \in \mathbb{R}^{\frac{H}{8} \times \frac{W}{4} \times D}$ are obtained by SVTR-B [11]. Subsequently, the flattened features denoted as $\text{ImgEmbs} \in \mathbb{R}^{\frac{H \cdot W}{32} \times D}$ are obtained by flattening the height (*h*) and width (*w*) of F_v and applying a layer normalization. Here, *D* represents the dimension of the features, and SVTR-B [11] sets it to 384.

Instruction Encoder

The instruction encoder comprises four learnable embeddings, as illustrated in Fig. 3. They are denoted as $CE \in \mathbb{R}^{C \times D}$, $PE \in \mathbb{R}^{P \times D}$, $FE \in \mathbb{R}^{F \times D}$, and $EE \in \mathbb{R}^{E \times D}$. Where *C*, *P*, *F*, and *E* signify the size of the character set, maximum position index, maximum character frequency, and existence (set to 2), respectively. The values of *P* and *F* are both set to *L*. These embeddings play a crucial role in generating $\text{CondEmbs} \in \mathbb{R}^{L_c \times D}$ and $\text{QuesEmbs} \in \mathbb{R}^{L_q \times D}$, as depicted in Fig. 3. The L_c and L_q are determined by the number of *Cond* and *Ques*.

Answer Head

The fusion of QuesEmbs , CondEmbs , and ImgEmbs is accomplished by CMFF. It yields AnsRelatedEmbs which is categorized into four groups according to *Ans*. Following this categorization, answer prediction is performed using the four heads depicted in Fig. 2. The resulting AnsPred is obtained through the softmax or sigmoid functions. The four heads are all linear classifiers, each associated with parameter matrices: $W_{rec} \in \mathbb{R}^{D \times C}$, $W_{fren} \in \mathbb{R}^{D \times F}$, $W_{check} \in \mathbb{R}^{D \times 1}$, and $W_{index} \in \mathbb{R}^{D \times P}$, respectively. Where *C*, *F*, and *P* are the same as the instruction encoder.

Algorithm 1: Pseudo-code of IGTR Pipeline in Python Style

```
import random
# text, image from training dataset
# ce: character-existence pairs of text
# cf: character-frequency pairs of text
# pc: position-character pairs of text
def RandomSplit(atrbs):
    p = random.randint(len(atrbs))
    random.shuffle(atrbs)
    return atrbs[p:], atrbs[:p]
def GenInstruction(ce, cf, pc):
    ceCond, ceQA = RandomSplit(ce)
    cfCond, cfQA = RandomSplit(cf)
    pcCond, pcQA = RandomSplit(pc)
    # generating cf attributes with constraint
    Cost = random.randint(2, len(text)-1) # constraint
    cfCostrntQA = GenCfCostrnt(text, Cost) if random.random() < 0.5 else []
    cfQA = cfQA + cfCostrntQA
    # grouping QA into four types by answer
    QARec, QAFreq, QACheck, QAindex = GenQAbyTask(ceQA, cfQA, pcQA, text)
    Ques = [QARec[:, 0], QAFreq[:, 0], QACheck[:, 0], QAindex[:, 0]] # question
    Ans = [QARec[:, 1], QAFreq[:, 1], QACheck[:, 1], QAindex[:, 1]] # answer
    Cond = [ceCond, cfCond, pcCond, GenSubString(text), len(text)] # condition
    return Cond, Ques, Ans # instruction
ImgEmbs = ImageEncoder(image)
K = 8
LossSum = 0
for k in range(K):
    Cond, Ques, Ans = GenInstruction(ce, cf, pc)
    CondEmbs, QuesEmbs = InstructionEncoder(Cond, Ques)
    AnsRelatedEmbs = CMFF(QuesEmbs, CondEmbs, ImgEmbs)
    AnsPred = ARec, AFreq, ACheck, AIndex = AnsHead(AnsRelatedEmbs, Ans)
    LossSum += AnswerLoss(AnsPred, Ans)
LossSum.backward() # back-propagate
update(IGTR) # AdamW
```

Answer Loss

The AnsPred is associated with its corresponding cross-entropy loss function. As a result, four losses are calculated and they are then summed to form a total loss \mathcal{L} according to the following formulas:

$$\begin{aligned}\mathcal{L}_{rec} &= CE_{Loss}(ARec, Ans[0]) \\ \mathcal{L}_{fren} &= CE_{Loss}(AFreq, Ans[1]) \\ \mathcal{L}_{check} &= BCE_{Loss}(ACheck, Ans[2]) \\ \mathcal{L}_{index} &= CE_{Loss}(AIndex, Ans[3]) \\ \mathcal{L} &= \mathcal{L}_{rec} + \mathcal{L}_{fren} + \mathcal{L}_{check} + \mathcal{L}_{index} \quad (1)\end{aligned}$$

6.3. The Illustration of Zero-shot Prediction

In Section 4.3, IGTR-Zero utilizes the character attribute prediction instruction only to understand text, thus establishing the zero-shot prediction capability. Fig. 5 provides a detailed illustration of the two instructions discussed in Tab. 6. These instructions rely on the length prediction and pre-task instructions initially to obtain information about the text’s length, as well as first and last characters (as the constraint, e.g., the second variable in the *constraint statistics* task, is set to larger than or equal to 2). Subsequently, the reasoning process depicted in Fig. 5 is employed to derive the recognition result.

For the *constraint statistics* task, we compile the character frequency at each constraint step. The character at the current step is determined by comparing the current

Algorithm 2: Pseudo-code of TS in Python Style

```
# rareCharList: characters appear less than 50 in training data
# simCharDict: dictionary of similarities for each character
def RandomSplit(atrbs):
    # generating attributes corresponding to the first 6 questions in Tab.1 for
    # randomly selected rare characters with 0/No answers.
    randomRareChar = random.sample(rareCharList, 3)
    randomRareCharAtrbs = GenCharAtrbs(randomRareChar, text, type(atrbs))
    rareAtrbs = []
    unrareAtrbs = []
    simCharsAtrbs = []
    for atrb in atrbs:
        char = atrb[0]
        # generating attributes corresponding to the first 6 questions in Tab.1
        # for randomly selected similar characters with 0/No answers.
        simChars = random.sample(simCharDict[char], random.randint(1, 3))
        simCharsAtrbs += GenCharAtrbs(simChars, text, type(atrbs))
        if char in rareCharList:
            rareAtrbs.append(atrb)
        else:
            unrareAtrbs.append(atrb)
    if len(rareAtrbs) >= 1 and random.random() < 0.75:
        CondAtrbs, QaAtrbs = unrareAtrbs, rareAtrbs
    else:
        p = random.randint(len(atrbs))
        random.shuffle(atrbs)
        CondAtrbs, QaAtrbs = atrbs[p:], atrbs[:p]
    return CondAtrbs, QaAtrbs + randomRareCharAtrbs + simCharsAtrbs
```

frequency change with the frequency of the previous step. In situations where multiple frequencies change simultaneously, the character with the highest predicted probability is selected as the inferred character. Concerning the *check character search* task, we validate the position of each character at the current step and obtain the corresponding binary classification answer. In cases where multiple characters receive a *Yes* answer, the one with the highest probability is chosen as the inferred character. Both instructions conclude the inference based on the predicted text length, leading to the final inferred text.

6.4. TS Instruction Generation in Section 4.4

The results presented in Tab. 7 and Tab. 8 demonstrate significant mitigation of the rarely appeared and morphologically similar character recognition problem through the application of the TS strategy. The primary philosophy of the TS strategy is to increase the sampling probability of the two kinds of characters. Its detailed procedure is outlined in Algorithm 2. In the context of Algorithm 1, `RandomSplit` can be substituted with Algorithm 2 when implementing the TS strategy.

Specifically, for rarely appeared characters, the count

of each character in the training set is examined. Characters occurring fewer than 50 times are aggregated in the rare character list (`rareCharList`), constituting approximately 55% of the character categories. The TS strategy employs two approaches to augment the sampling probability based on `rareCharList`. Firstly, three characters are randomly selected from `rareCharList`, and their corresponding character attributes are generated using `GenCharAtrbs`. These attributes are then merged with `QaAtrbs`. Secondly, if rare characters are presented in the current text, there is a probability of 75% that the attributes of the rare characters will be utilized as `QaAtrbs`, while the attributes of the non-rare characters will be designated as `CondAtrbs`.

As for morphologically similar characters, firstly, the confusion matrix of IGTR-PD prediction results, without employing the TS strategy, is obtained. The top three characters of incorrect predictions for each character constitute its similar character dictionary (`simCharDict`). When generating `QaAtrbs`, 1-3 similar characters are randomly chosen from `simCharDict` for each character in the attributes. `GenCharAtrbs` is then applied to create the corresponding similar character attributes, which are sub-

GT: shanghaizhiweicenturyhotel	GT: dongpumarketingservicecenter
PD: shanghaizhiweicenturyotl	PD: dongpumarketingservicecer__
AR: shanghaizhiweicentury__	AR: dongpumarketingservicece__
Next: shanghaizhiweicenturyhotel	Next: dongpumarketingservicecenter
GT: mildfoamcleansercontaining	GT: shandandancursinenorthwest
PD: mildfoamcleansercontai_ing	PD: shandandancursinenortw_st
AR: mildfoamcleansercontainin_	AR: shandandancursine_____
Next: mildfoamcleansercontaining	Next: shandandandandandandand...

Figure 6. The recognition results of three kinds of decoding methods for long texts. Incorrect predictions are marked in red and missed predictions are denoted as underlined.

sequently merged with $QaAttrbs$. For instance, if the current attribute is framed as the question “*Is the i -th character 大?*” and the answer is *Yes*, then a similar character attribute is generated as the question “*Is the i -th character 太?*” and the answer is *No*. This methodology ensures that the attributes of similar characters associated with each character in the question-answer pair are concurrently used to enhance IGTR’s capability to recognize morphologically similar characters.

It is important to note that $GenCharAttrbs$ selectively chooses available question-answers for generation. It focuses on the first six questions in Tab. 1 involving character variables based on the current attribute type. This refinement streamlines the process and ensures its relevance to the ongoing attribute type considerations.

7. More Experiments and Analysis

7.1. Re-identification and Extrapolating Recognition

In Tab. 2, four distinct recognition instructions are implemented. The first two (PD and AR) correspond to prevailing decoding methods in previous approaches. The re-identification (RI) instruction aligns with in ABINet [14] and PARSeq [3], offering a mechanism to rectify inaccurately predicted results. Further, we applied the RI instructions after the PD instructions to correct the possible misrecognition, and the corresponding results (IGTR-PD-RI) are presented in Tab. 12. The results indicate that this correction leads to improvements in most benchmarks, demonstrating the effectiveness of the RI instructions.

In PD and AR methods, typically, learnable position embeddings ($\in \mathbb{R}^{L \times D}$) are pre-set, where L denotes the maximum recognition text length. This limitation implies that PD and AR are incapable of handling text with more than L characters. In order to overcome this limitation, the extrapolation recognition (ER) instruction is proposed. It employs a

sub-string as the condition without requiring the pre-set position embeddings. ER requires the IGTR model to match the sub-string in the text image. Subsequently, the next/previous character of the sub-string is determined. Taking *ARTETA* as an illustration, if a condition of ER is “*There is a sub-string $RTET$ ”* with a question being “*What is the next character of the sub-string?*”. The IGTR model firstly matches *RTET* in the text image, followed by identifying the next character of the sub-string as *A*. Consequently, ER can theoretically recognize text of any length, despite being trained on text images within L characters.

Aiming to validate ER (with a sub-string of length 5), we initially followed the experimental methods of PD and AR to obtain its results (IGTR-Next) on benchmarks, as shown in Tab. 12. And then, we worked with four long texts from Union14-L [22] to verify whether ER can recognize a text exceeding L characters. The recognition results are illustrated in Fig. 7. The results demonstrate that IGTR-Next performs exceptionally well even without the position embeddings. Additionally, three examples of successfully recognized long texts illustrate that IGTR-Next excels in the length extrapolation recognition task, both highlighting its potential as a novel recognition method. The error in the fourth example is caused by the repetition of the same sub-string in the text image, resulting in circular recognition. This can be considered an inherent limitation of IGTR-Next. Increasing the length of the sub-string helps alleviate this flaw.

Nevertheless, it is noteworthy that all four recognition methods are unified into the proposed instruction-guided scheme without additional structure, further emphasizing the superiority of IGTR as a novel paradigm for STR.

7.2. Comparison with State-of-the-Art

Particularly, SVTR-B, equipped with a rectification module (STN [45]), achieves the best results to date on Union14M-L [22] benchmarks. To ensure a fair comparison with other methods, IGTR utilizes the SVTR-B backbone (with STN and the CTC decoder removed) as the image encoder. The results of SVTR-B without STN are presented in Tab. 12. Nevertheless, IGTR outperforms SVTR-B and other methods. Specifically, with regard to curve and multi-oriented benchmarks which are characterized by extreme irregularities, the previous approaches often misidentify challenging text images in both benchmarks due to misfocusing on difficult characters. On the contrary, IGTR easily achieves accurate recognition by leveraging its ability to comprehend character attributes. This observation underscores that IGTR excels in achieving a deeper understanding of the fine-grained content of text images through the proposed instruction-guided scheme, thereby gaining a significant advantage in text recognition.

When evaluating performance on Chinese benchmarks

Method	Common Benchmarks							Union14M-L Benchmarks							Parameters ($\times 10^6$)	
	IC13	SVT	IIIT	IC15	SVTP	CUTE	Avg	Curve	Multi-Oriented	Artistic	Contextless	Salient	Multi-Words	General		Avg
SVTR-B [11]	97.1	91.5	96.0	85.2	89.9	91.7	91.90	69.8	37.7	47.9	61.4	66.8	44.8	61.0	55.63	24.6
SVTR-B [11] w/o STN	97.3	94.1	96.4	86.7	90.7	91.0	92.71	58.6	15.0	50.9	58.3	67.3	60.2	62.0	53.18	18.1
IGTR-PD	97.6	95.2	97.6	88.4	91.6	95.5	94.30	76.9	30.6	59.1	63.3	77.8	62.5	66.7	62.40	24.1
IGTR-AR	98.6	95.7	98.2	88.4	92.4	95.5	94.78	78.4	31.9	61.3	66.5	80.2	69.3	67.9	65.07	24.1
IGTR-PD-RI	97.7	95.5	97.7	88.5	91.6	95.5	94.43	77.3	31.0	59.6	64.3	78.4	65.9	67.2	63.40	24.1
IGTR-Next	97.3	94.9	97.2	88.3	91.7	95.1	94.09	78.2	32.0	60.6	59.1	78.2	57.8	67.1	61.84	24.1
SVTR-B [11]	97.5	96.4	97.8	89.3	91.0	96.2	94.72	85.4	87.4	68.9	79.5	84.3	79.1	81.8	80.91	24.6
SVTR-B [11] w/o STN	97.5	97.8	98.1	89.0	91.3	95.1	94.82	75.2	46.2	69.2	76.9	73.5	76.1	79.2	70.89	18.1
IGTR-PD	97.7	97.7	98.3	89.8	93.7	97.9	95.86	88.1	89.9	74.2	80.3	82.8	79.2	83.0	82.51	24.1
IGTR-AR	98.1	98.4	98.7	90.5	94.9	98.3	96.48	90.4	91.2	77.0	82.4	84.7	84.0	84.4	84.86	24.1
IGTR-PD-RI	97.8	97.8	98.3	89.7	93.8	97.9	95.91	88.6	90.0	74.1	80.6	83.2	79.9	83.5	82.86	24.1
IGTR-Next	98.1	97.8	98.3	90.5	94.0	97.2	95.99	89.4	92.3	76.2	78.9	84.7	80.9	84.0	83.78	24.1

Table 12. IGTR series are not equipped with STN [45], and for a clearer analysis of the IGTR gains, the results of SVTR-B without STN [45] are presented. The top and bottom parts present the results of training on the synthetic and the Union14M-L [22] dataset, respectively.



Figure 7. The predictions of IGTR.

[6], IGTR exhibits consistent advantages (see Tab. 11). The significant long-tailed distribution of Chinese characters contributes to a pronounced overfitting phenomenon, with a training accuracy reaching 99.2%, despite IGTR’s ability to generate rich instructions. Therefore, we employ the same data augmentation strategy as applied to the English model, resulting in a final training accuracy of 84%. Remarkably, this approach not only mitigates the overfitting but also enhances IGTR’s performance on the four Chinese benchmarks [6] (see Tab. 11).

Additionally, the inference process (PD and AR) of IGTR and the prediction results for extremely challenging samples are illustrated in Fig. 7. As shown in Fig. 7(a-i), IGTR successfully (✓) recognizes these instances, where most of the previous methods failed. The bad (x) cases

(j,k,l) are quite challenging even for humans, and the attribute prediction and recognition results also show where it makes mistakes.